Available online at www.sciencedirect.com

ScienceDirect

journal homepage: http://www.elsevier.com/locate/rpor

Original research article

A closer look at the conventional Winston-Lutz test: Analysis in terms of dose

Juan-Francisco Calvo-Ortega[a,b,*], *Sandra Moragues-Femenía*[a,b], *Coral Laosa-Bello*[a,b], *Sol San José-Maderuelo*[a,b], *Joan Casals-Farran*[a,b]

[a] *Servicio de Oncología Radioterápica, Hospital Quirónsalud, Barcelona, Spain*
[b] *Servicio de Oncología Radioterápica, Hospital Universitari Dexeus, Barcelona, Spain*

ARTICLE INFO

Article history:
Received 22 November 2018
Received in revised form
27 April 2019
Accepted 6 July 2019
Available online 18 July 2019

Keywords:
Winston-Lutz
SRS
Radiochromic

ABSTRACT

Aim: To investigate whether the target-isocenter deviations reported by a conventional Winston-Lutz (WL) test actually reflect the shifts of the measured prescription isodose line with respect to the target.

Background: A conventional WL test uses a metallic ball as a target that aims at several fields. But this test does not report information on the accuracy of the delivery in terms of dose.

Materials and methods: A conventional WL test using a metallic pointer as a target (Pointer-WL test) has been recreated in the Eclipse treatment planning system over an acrylic phantom containing a radiochromic film (Dose-WL test). After Dose-WL test delivery, the shift of the 80% prescription isodose line with respect to the target center (d80%-center) was measured using film dosimetry. The Pointer-WL and Dose-WL tests were performed in 10 different sessions. The isocenter deviation reported by the Pointer-WL test was compared to the d80%-center vector, according to the three patient's directions (Left–Right or LR; Anterior–Posterior or AP; and Superior–Inferior or SI).

Results: The deviations (mean ± SD) found for the Dose-WL tests (LR: 0.5 ± 0.4 mm; AP: 0.5 ± 0.4 mm; SI: 0.6 ± 0.2 mm) were in most cases less than 1 mm, and they were significantly smaller (all $p < 0.05$) than the maximum deviations reported by the Pointer-WL tests (LR: 1.3 ± 0.3 mm; AP: 1.2 ± 0.4 mm; SI: 1.1 ± 0.3 mm).

Conclusions: The Dose-WL test described in this study allows estimating the spatial accuracy of the prescription isodose line.

1. Background

Stereotactic radiosurgery (SRS) is a non-surgical radiotherapy procedure for the treatment of both benign and malignant lesions of the brain.[1] Intracranial SRS was initially developed in the 1960s using a Gamma Knife platform, but a standard linear accelerator (linac) modified for stereotactic purposes has been an alternative approach to Gamma Knife SRS since the 1980s.[2] The Winston-Lutz (WL) test is a well-described procedure developed for verification of the linac isocenter for cranial SRS.[3] A small metallic ball phantom, which is representative

* *Corresponding author at*: Departamento de Oncologia Radioterápica, Hospital Quirónsalud, Plaza Alfonso Comín, 5-7, 08023 Barcelona, Spain.
E-mail address: jfcdrr@yahoo.es (J.-F. Calvo-Ortega).
https://doi.org/10.1016/j.rpor.2019.07.003
1507-1367/

of the planned target, is fixed to the linac couch by a locking mechanism. The ball center is positioned at the linac isocenter defined by the lasers of the treatment room. The ball is then irradiated with several beams at different angulations of the gantry and couch, and each shot is imaged using a film placed perpendicular to the beam direction on a stand behind ball, or using the electronic portal imaging device (EPID) of the linac. The measured distances for all shots between the center of the ball shadow and the radiation field center reveal isocenter movements. Ideally, differences should be less than 1 mm to avoid important dose errors during the treatment delivery.[4]

Classically, SRS has relied on an invasive head frame for patient immobilization and target localization. In recent years, the irruption of the image-guided radiotherapy (IGRT) has enabled the practice of non-invasive (frameless) radiosurgical treatments.[5] For instance, the cone-beam computed tomography (CBCT) technology available on the modern day linacs allows acquiring 3D images of the patient's head in the treatment position.[6] Jones et al. have developed an imaged-guided WL test that evaluates errors in CBCT-based setups.[7] This test is intended to check the CBCT-based ball phantom alignment with the radiation treatment isocenter by following the clinical IGRT workflow. In this way, the imaged-guided WL considers several inaccuracy sources as CBCT isocenter/MV isocenter alignment, CBCT-based registration software, remote linac couch motions and the multileaf collimator (MLC) positional accuracy. In this article, we will be referring to the conventional ball-based WL test with or without IGRT as a Pointer-WL test.

However, the Pointer-WL test does not provide information on the geometrical accuracy of the delivery in terms of dose, which is the quantity of interest in radiotherapy. In this study we describe a dosimetric WL test performed using radiochromic films (Dose-WL test). We aim to investigate whether the deviations revealed by the Pointer-WL actually reflect the geometrical shifts of the measured prescription isodose line with respect to the target center reported by the Dose-WL test. In other words, we attempt to explain the pitfalls of the Pointer-WL test used for cranial stereotactic QA procedure in comparison with dose-based geometric shift estimation.

2. Aim

The purpose of the present study is to analyze the dosimetric impact of the deviations revealed by a conventional WL test consisting in targeting a ball phantom. In order to investigate whether these deviations actually reflect the shift of the measured prescription isodose line in respect to the target center, a phantom containing a radiochromic film was used.

3. Materials and methods

3.1. *Pointer-WL test*

The Pointer-WL test was implemented in 2011 in our department following the methodology described by Jones et al.,[7] but using the BrainLAB Winston-Lutz pointer phantom (BrainLAB AG, Munich, Germany) in the form of a 5 mm-diameter tungsten ball embedded in a plastic structure (Fig. 1). The plastic cover has marks on it showing the center of the ball to facilitate an easy visual setup. Axial CT images of the phantom were acquired with a 1 mm slice distance in an Optima CT660 scanner (GE Medical Systems, Waukesha, WI), and then transferred to the Eclipse v. 13.6 TPS (Varian Medical Systems, Palo Alto, USA). The tungsten ball was outlined and a WL plan consisting of 15 non-coplanar fields (6 MV photons) was created with the isocenter located at the ball center. A square aperture of 2 cm × 2 cm for each beam was defined using the central leaves of the Millennium 120 MLC of a Varian Clinac 2100 CD. The following gantry (G) and couch (C) positions were used: G140C0, G90C0, G40T0, G0C0, G320C0, G270C0, G220C0, G180C0, G300C315, G240C315, G120C45, G60C45, G150C90, G115C90 and G20C90, where the angles are given in degrees according to the Varian IEC 601-2-1 scale. Collimator rotation angle was not varied because all SRS treatments are planned in our clinical routine with collimator at the zero-degree position. Five monitor units (MU) were programmed for each field. In addition, a kV-CBCT setup field was included in this plan to be acquired using the Varian On-Board Imaging (OBI) system of the linac. The WL plan was activated in the Aria v 13.6 record and verify system (Varian Medical Systems, Palo Alto, USA) for delivery.

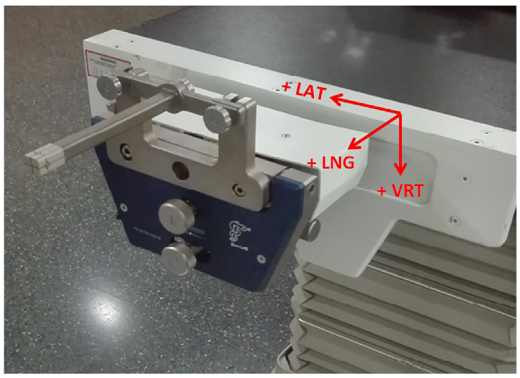

Fig. 1 – The BrainLAB pointer phantom attached to the linac couch using the BrainLAB couch-mount device. The translational movements (LNG, LAT and VRT) of the couch are shown.

The BrainLAB pointer phantom was attached to the linac couch using the couch-mounted adaptor provided by BrainLAB. Following the methodology described by Jones et al.,[7] once the pointer phantom was aligned using the in-room lasers, intentional random shifts within ±5 mm were applied in the longitudinal (LNG), lateral (LAT) and vertical (VRT) directions of the linac couch (Fig. 1). In this way, inaccuracies associated with IGRT software alignment and remote couch motions will be taken into account in the Pointer-WL test. Then, the pointer was CBCT scanned with the protocol used in our department for SRS treatments (Pelvis mode: half-fan technique, 125 kVp, 680 mAs, 360 mm field of view, 384 × 384 matrix; 1 mm slice distance). Pelvis mode is the highest-quality image protocol available in our OBI system.[8] The 3D/3D match tool on the OBI workstation v. 1.6 was used to manually align the acquired CBCT with the planning CT. The manual registration focused on the tungsten ball, and the resulting

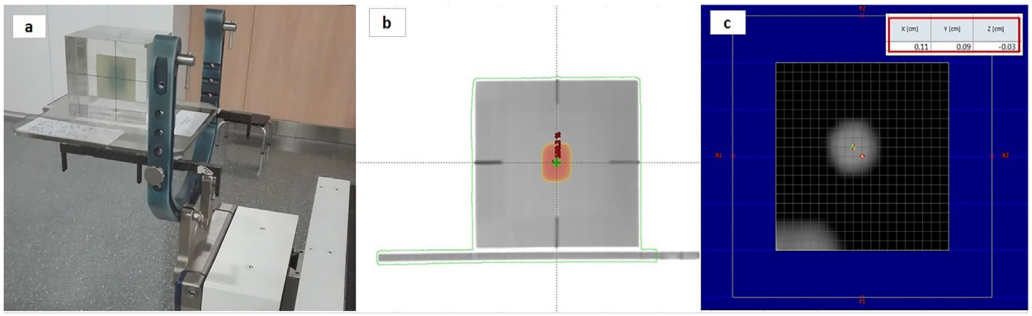

Fig. 2 – Sagittal acrylic phantom used in this study (a); cross-hair of the Eclipse TPS (dotted lines) is used to place the isocenter of the WL plan at the point defined by the four fiducial marks of the coronal phantom. In orange color is represented the 80% isodose area (b); (c) example of isocenter 3D recreation: 1 mm d_{ball_field} deviations detected in the EPID image acquired for a non-coplanar field were simulated using the Eclipse's BEV tool. MLC is displayed in blue color, the yellow-green-red cross-hair is the ball center; the red circle is the field isocenter; and a 1 mm grid size is displayed. The X1–X2 and Y1–Y2 axes coincide with the transversal and longitudinal directions of the EPID. X–Y–Z shifts according to the patient's coordinate systems were derived (see red square: X is LR, Y is AP and Z is SI).

shifts required by the 3D/3D match were remotely applied via couch motions. Finally, the pointer phantom was irradiated with the 2 cm × 2 cm Winston-Lutz fields of the WL plan. Each shot was imaged using the EPID (Varian aSi 500 II) of the linac, with a source-to-imager distance of 180 cm giving a pixel size of 0.4 mm × 0.4 mm at the isocenter plane.

3.2. *Dose-WL test*

Two home-made phantoms were used. Each consisted of two acrylic blocks of 10 cm × 10 cm × 5 cm such that a film piece of 5 cm × 5 cm may be sandwiched between the blocks. Four linear radio-opaque copper marks of 0.1 mm-diameter defining a virtual cross-hair were engraved in the block intended to support the film. Both phantoms were glued to plastic trays: one phantom was positioned in a coronal orientation (*coronal phantom*), while the other one was in a sagittal position (*sagittal phantom*). For each case, the final assembly was attached to the BrainLAB U-ring by mimicking the setup used for our cranial SRS treatments (Fig. 2a).

Each phantom without a film was CT scanned with a 1 mm slice distance with an Optima CT660 scanner. The CT images were transferred to the Eclipse TPS and the four radio-opaque marks were identified. The center of the cross-hair passing through the marks was set as the origin of the CT image volume (Fig. 2.b). An uncertainty of 0.2 mm ($k = 1$) selecting this origin was estimated as the standard deviation in DICOM coordinates of the origin points obtained by two users from repeated origin selections. The same WL plan designed for the BrainLAB pointer phantom was created for the coronal and sagittal phantoms, but 30 MU were computed for all fields to give a maximum dose around 3 Gy at the film plane. The Analytical Anisotropic Algorithm (AAA) v. 10.0.28 of the Eclipse TPS was used for dose calculation with a 1.0 mm grid size. The isocenter was placed at the origin previously established in the Eclipse TPS. In this way, when a coronal/sagittal dose plane passing through the origin for the coronal/sagittal phantom was exported, the dose matrix center matched with the planned isocenter. In this study, we used dose matrices of 10 cm × 10 cm and 512 × 512 pixels (0.2 mm/pixel). The WL plan was activated in the Aria record and verify system for delivery.

For the WL plan delivery, each phantom loaded with a 5 cm × 5 cm film was initially set up by aligning its four radio-opaque marks with the room lasers. As it was done for the Pointer-WL test, intentional and arbitrary misalignments within ±5 mm were manually applied to the phantom using translational movements of the couch. As our linac couch is not able to correct roll and swivel rotations, no rotation errors were forced to the phantom. Rotational errors are addressed in our clinical practice with an online adaptive procedure designed in our department requiring only translational corrections.[9] The final image-guided phantom setup was done by acquiring CBCT images using the Pelvis protocol. The match was focused on the four radio-opaque marks which are visible in both scans. In order to correct the phantom position, the needed shifts were remotely applied, i.e., using couch auto-shifting from the linac console outside the treatment room. After that, the WL plan was delivered without performing image-guided corrections after each couch kick. Once the WL plan irradiation was finished, the 5 cm × 5 cm film was removed and kept out of the light to be scanned after twenty hours of exposure.

3.3. *Film dosimetry*

The dosimetry system used in this study consisted of: (a) Gafchromic EBT3 films (8×10F model, Ashland Specialty Ingredients, Advanced Materials Group, Wayne, NJ); (b) a flatbed Epson V750 Pro color scanner (Epson Seiko Corporation, Nagano, Japan); and (c) the triple-channel method implemented in the Radiochromic.com v. 3.0.10 cloud-based software (https://radiochromic.com) for radiochromic film dosimetry.[10]

The EBT3 film pieces of 5 cm × 5 cm were obtained from a single batch (Lot #10251701). All the film pieces were labeled and tracked by using permanent ink marks to keep the portrait orientation of the whole film in the pieces extracted from it. Four fiducial marks along the cross-hair passing through the four radio-opaque marks of the phantom were outlined with a

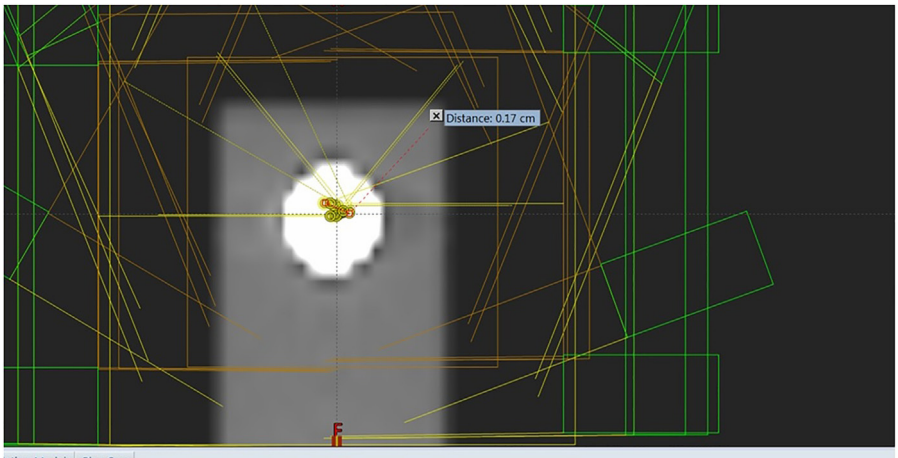

ation Models | Plan Sum

Gantry Rtn [deg]	Coll Rtn [deg]	Couch Rtn [deg]	Wedge	Field X [cm]	X1 [cm]	X2 [cm]	Field Y [cm]	Y1 [cm]	Y2 [cm]	X [cm]	Y [cm]	Z [cm]
140.0	0.0	0.0	None	3.0	+1.5	+1.5	3.0	+1.5	+1.5	0.05	-0.04	0.03
90.0	0.0	0.0	None	3.0	+1.5	+1.5	3.0	+1.5	+1.5	0.00	-0.08	0.05
40.0	0.0	0.0	None	3.0	+1.5	+1.5	3.0	+1.5	+1.5	-0.03	-0.03	0.09
0.0	0.0	0.0	None	3.0	+1.5	+1.5	3.0	+1.5	+1.5	0.01	0.00	0.10
320.0	0.0	0.0	None	3.0	+1.5	+1.5	3.0	+1.5	+1.5	0.02	-0.02	0.09
270.0	0.0	0.0	None	3.0	+1.5	+1.5	3.0	+1.5	+1.5	0.00	-0.07	0.04
220.0	0.0	0.0	None	3.0	+1.5	+1.5	3.0	+1.5	+1.5	-0.06	-0.05	0.03
180.0	0.0	0.0	None	3.0	+1.5	+1.5	3.0	+1.5	+1.5	-0.04	0.00	0.02
300.0	0.0	315.0	None	3.0	+1.5	+1.5	3.0	+1.5	+1.5	0.04	-0.02	0.02
240.0	0.0	315.0	None	3.0	+1.5	+1.5	3.0	+1.5	+1.5	-0.06	-0.12	0.04
120.0	0.0	45.0	None	3.0	+1.5	+1.5	3.0	+1.5	+1.5	0.02	-0.08	0.05
60.0	0.0	45.0	None	3.0	+1.5	+1.5	3.0	+1.5	+1.5	-0.05	-0.04	0.02
150.0	0.0	90.0	None	3.0	+1.5	+1.5	3.0	+1.5	+1.5	0.12	-0.05	0.09
115.0	0.0	90.0	None	3.0	+1.5	+1.5	3.0	+1.5	+1.5	0.09	-0.13	0.06
20.0	0.0	90.0	None	3.0	+1.5	+1.5	3.0	+1.5	+1.5	0.04	0.04	0.10

Fig. 3 – Resulting isocenter "cloud" after mimicking the d_{ball_field} deviations reported by a Pointer-WL test. Each reconstructed isocenter is represented in the figure by a yellow circle. In the red square are shown the 3D coordinates of each isocenter with respect to the ball center (X is LR, Y is AP and Z is SI).

permanent ink within ±0.2 mm in each film. A sensitometric curve to convert film pixel values to doses was established between 0 and 5 Gy for the batch of films used in this study.

All exposed films were digitized on the Epson V750 Pro flatbed scanner twenty hours after irradiation. The scanner was warmed-up for 30 min before use. Scanning was performed in a transmission mode at 48-bit RGB (16 bits per color channel) and with a spatial resolution of 72 dpi. The acquired images were saved as uncompressed TIFF files. Each piece of the film was positioned in the center of the scanner plate using a transparent glass on top of the film to avoid curling during scanning.[11] Before scan acquisitions, and after pauses, five successive blank scans were performed to stabilize the scanner lamp. All pieces of the film were scanned five times and only the last four readings were included in the dosimetric analysis.

3.4. *Data analysis*

For the Pointer-WL test analysis, the distance between the centers of the ball shadow and the radiation field at the isocenter plane (d_{ball_field}) was measured in every EPID image acquired during the WL plan delivery. An in-house macro developed in Image J v. 1.51s (NIH, Bethesda, MD) was used for this task.[12] The accuracy of this macro to determinate the d_{ball_field} distance was estimated as 0.1 mm. For each field of the WL plan, the horizontal and vertical components (in the pixel-based coordinate system of the EPID) of the d_{ball_field} vector were simulated in the Eclipse by using the beam's eye view (BEV) tool such that the actual 3D position of the radiation isocenter may be recreated (Fig. 2c). So, the shifts of the radiation center with respect to the ball center were derived along the three patient's axes (Left–Right or LR; Anterior–Posterior or AP; and Superior–Inferior or SI) for all fields of the WL plan (Fig. 3). For each direction, the absolute maximum shift among all fields of the WL plan was considered as the targeting error in that direction ($d_{ball\_field\_max}$). Also, the mean shift (in absolute value) for each direction was analyzed ($d_{ball\_field\_mean}$).

For the Dose-WL test, each film image (one for the coronal phantom and the other for the sagittal phantom) was imported into the Radiochromic.com application to be converted into a dose image. The dose image was segmented using the thresholding tool of Image J to extract the dose area corresponding to 80% of the dose value of the central point defined by the four pen marks (Fig. 4a). An 80% dose level was selected as this is typically the prescription isodose line used in our SRS treatments. It is noteworthy that the WL plan computed by Eclipse has the property that the center of the 80% isodose area matches with the planned isocenter both for the coronal and sagittal planes. After applying the binary filter of Image J, the centroid of the 80% dose area was obtained (Fig. 4b).

Once the centroid of the 80% dose is derived, it is necessary to locate the planned isocenter on the dose image. This isocenter represents the center of a virtual target volume treated with the WL plan. The center of the virtual cross-hair passing through the four pen marks is a surrogate of the planned isocenter. To locate the isocenter, the centroid of each pen mark was determined on the image by using a binary filter (Fig. 4b). Then, the intersection point of the two straight lines passing through the paired centroids was calculated. Finally, the three-dimensional deviation ($d_{80\%\_center}$) between

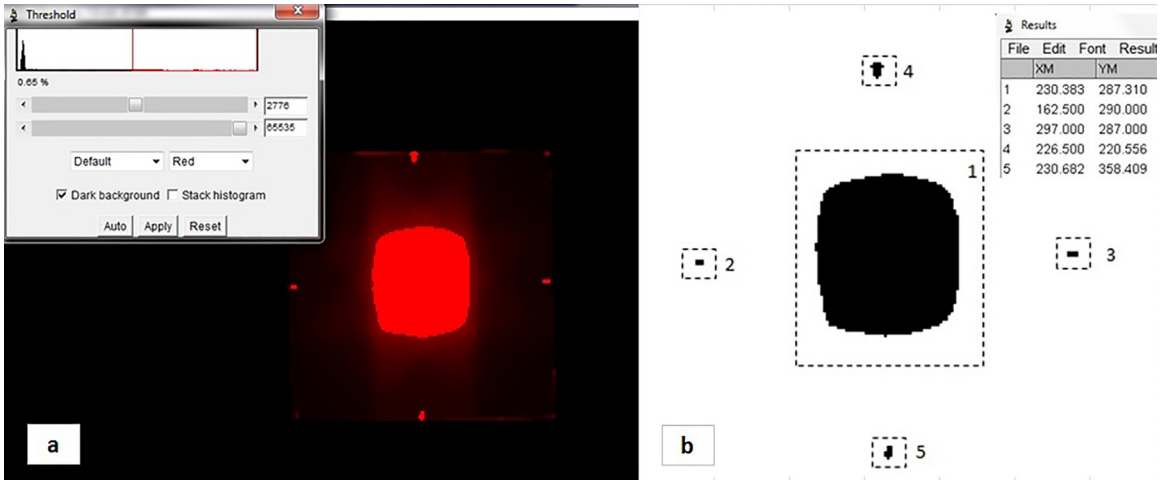

Fig. 4 – Film image is analyzed with Image J software: (a) thresholding to detect the 80% dose area; and (b) a binary filter is applied to the resulting image. Center of mass coordinates (XM and YM, in pixels units) are calculated in five regions of interest (dotted lines): one is placed over the 80% dose area and the others over the four pen marks. From these data, the deviation (Euclidean distance) between the radiation center and the planned isocenter is derived.

this intersection point (planned isocenter) and the centroid of the 80% dose area was calculated for the two irradiated films on each test (one using the coronal phantom and the other with the sagittal phantom). So, $d_{80\%\_center}$ represents the targeting accuracy. The components of the $d_{80\%\_center}$ vector along the patient's axes (LR, AP, and SI) were derived as well. The SI deviation was averaged from the two values measured at both films.

The $d_{ball\_field\_max}$ and the $d_{80\%\_center}$ metrics were compared for paired Pointer-WL and Dose-WL tests delivered over 10 different sessions. Statistical significance of each comparison was evaluated using a 2-tailed Student t-test. Differences were reported as statistically significant at the $p < 0.05$ level.[13] Same type of comparative analysis was carried out for $d_{ball\_field\_mean}$ and $d_{80\%\_center}$.

For each session, one Pointer-WL test with the BrainLAB pointer phantom, one Dose-WL test with the coronal phantom and one Dose-WL test with the sagittal phantom were delivered. The same intentional misalignments were applied to the three phantoms. We want to emphasize that the validation of the shifts determined by CBCT registration is not an aim of this study. Therefore, the corrective CBCT-derived shifts will not be compared with the intentional random shifts applied to any phantom used in this study before being CBCT scanned.

4. Results

Table 1 shows the absolute values found for the $d_{ball\_field\_max}$ and $d_{80\%\_center}$ metrics in each anatomical patient's direction (LR, AP, and SI) for the ball-based Pointer-WL and the film-based Dose-WL tests, respectively. The deviations (mean ± SD) found for the Dose-WL tests (LR: 0.5 ± 0.4 mm; AP: 0.5 ± 0.4 mm; SI: 0.6 ± 0.2 mm) were in most cases less than 1 mm, and they were significantly smaller (all $p < 0.05$) than the maximum deviations reported by the Pointer-WL tests (LR: 1.3 ± 0.3 mm; AP: 1.2 ± 0.4 mm; SI: 1.1 ± 0.3 mm). Only one deviation ≥ 1 mm was observed for the Dose-WL tests. On average, $d_{ball\_field\_max}$ exceeded 0.8 mm (in RL direction), 0.7 mm (in AP direction) and 0.5 mm (in SI direction) the $d_{80\%\_center}$ deviations. In contrast, no statistically significant difference was found in any anatomical patient's direction between the $d_{ball\_field\_mean}$ and $d_{80\%\_center}$ (Table 2).

The uncertainty values (U; with $k = 1$) for each metric were: $U = 0.2$ mm for $d_{ball\_field\_max}$ and $d_{ball\_field\_mean}$, and $U = 0.1$ mm for $d_{80\%\_center}$. They were estimated as the standard deviation in measured results from several experiments of each test type.

We attempted to explain the pitfalls of the traditional Pointer-WL test for cranial stereotactic QA procedure in comparison with dose-based geometric shift estimation. A dosimetric WL test (Dose-WL test) performed using radiochromic films has been described and we have analyzed the shifts between the measured 80% prescription isodose line and the target center. As far as we know, a dosimetric WL test has not been described before in the literature for linac-based SRS QA. A similar procedure was described by Ma et al. but using a Gamma Knife unit.[14] Differently to the conventional WL test, they determined on a film the absolute shifts between the radiation center defined by a peripheral isodose band (~40–60% of the central dose) and the center of a pin marker used as a target.

In this study, we showed the disconnective outcome of the geometrical shift estimations from the conventional Pointer-WL test ($d_{ball\_center\_max}$) with delivered dose variation reported by the corresponding Dose-WL test ($d_{80\%\_center}$). Our results show that large deviations detected by the Pointer-WL test (values of $d_{ball\_center\_max}$ up to 1.9 mm) did not imply, in general, errors larger than 1 mm along the patient's axes as revealed by the Dose-WL test designed in this study (Table 1). This dosimetric test reported submillimeter average deviations of 0.5 mm in the LR and AP directions, and 0.6 mm along the SI direction.

Table 1 – Deviations found along the patient's direction (LR, AP, SI) for each type of test: $d_{ball\_field\_max}$ is the absolute maximum deviation registered among the 15 EPID images of a given Pointer-WL test, while $d_{80\%\_center}$ deviations are reported by the corresponding Dose-WL tests. All deviations are in millimeters. For each test, the shifts applied along the LNG, LAT and VRT directions of the linac couch are specified (Fig. 1).

# Test (LNG,LAT,VRT)	LR		AP		SI	
	$d_{ball\_field\_max}$	$d_{80\%\_center}$	$d_{ball\_field\_max}$	$d_{80\%\_center}$	$d_{ball\_field\_max}$	$d_{80\%\_center}$
#1 (+3, +3,+3)	1.2	0.8	1.3	0.5	1.0	0.5
#2 (−2,−2,−2)	1.5	0.1	0.6	1.0	0.8	0.6
#3 (+1,+1,+1)	1.1	0.1	1.5	0.0	1.5	0.3
#4 (+5,+5,+5)	1.1	0.5	0.6	0.9	1.2	0.2
#5 (−2/−3/−1)	0.9	0.7	1.0	1.0	1.3	0.5
#6 (−2,+4,−2)	1.9	0.4	0.6	0.0	0.9	1.0
#7 (0,0,0)	1.8	0.5	1.3	0.1	1.8	0.6
#8 (+2,−4,+2)	1.6	0.8	1.6	0.6	0.9	0.5
#9 (+1,+2,+3)	1.1	1.3	1.3	0.0	0.7	0.9
#10 (+2,+3,+1)	1.2	0.3	1.8	0.6	0.9	0.6
Mean	1.3	0.5	1.2	0.5	1.1	0.6
SD	0.3	0.4	0.4	0.4	0.3	0.2
p-Value	0.0007		0.0053		0.0040	

Table 2 – Deviations found along the patient's direction (LR, AP, SI) for each type of test: $d_{ball\_field\_mean}$ is the absolute average deviation registered among the 15 EPID images of a given Pointer-WL test, while $d_{80\%\_center}$ deviations are reported by the corresponding Dose-WL tests. All deviations are in millimeters. For each test, the shifts applied along the LNG, LAT and VRT directions of the linac couch are specified (Fig. 1).

# Test (LNG,LAT,VRT)	LR		AP		SI	
	$d_{ball\_field\_mean}$	$d_{80\%\_center}$	$d_{ball\_field\_mean}$	$d_{80\%\_center}$	$d_{ball\_field\_mean}$	$d_{80\%\_center}$
#1 (+3,+3,+3)	0.1	0.8	0.5	0.5	0.6	0.5
#2 (−2,−2,−2)	0.4	0.1	0.0	1.0	0.1	0.6
#3 (+1,+1,+1)	0.4	0.1	0.3	0.0	0.9	0.3
#4 (+5,+5,+5)	0.2	0.5	0.2	0.9	0.5	0.2
#5 (−2/−3/−1)	0.2	0.7	0.2	1.0	0.4	0.5
#6 (−2,+4,−2)	0.6	0.4	0.0	0.0	0.3	1.0
#7 (0,0,0)	0.3	0.5	0.6	0.1	0.9	0.6
#8 (+2,−4,+2)	0.7	0.8	0.5	0.6	0.4	0.5
#9 (+1,+2,+3)	0.3	1.3	0.2	0.0	0.0	0.9
#10 (+2,+3,+1)	0.1	0.3	0.7	0.6	0.4	0.6
Mean	0.3	0.5	0.3	0.5	0.4	0.6
SD	0.2	0.4	0.2	0.4	0.3	0.2
p-Value	0.1472		0.3862		0.4457	

We think the spatial deviation of radiation isocenter estimated by the $d_{ball\_field\_max}$ metric of the Pointer-WL test will not agree with the isodose shifts reported by a planar dosimetric analysis ($d_{80\%\_center}$) when the same irradiation geometry is used (see Table 1). We argue that the spatial discrepancy due to each field loses its individual representation when the dose from all fields of the WL plan is delivered in a film. In other words, the accumulated planar dose is not sensitive to represent the radiation isocenter deviations associated with the individual fields. This assumption is also supported by the results shown in Table 2: the isocenter shifts of the 15 fields of the WL plan partially compensate each other, resulting in not statistically significant difference between $d_{ball\_field\_mean}$ and $d_{80\%\_center}$, with the values of both metrics being smaller than the deviation reported by the classical analysis of the WL test ($d_{ball\_field\_max}$).

In a previous investigation performed in our department, the geometrical deviations resulting from 15 Pointer-WL tests were simulated field by field over 5 cranial SRS cases.[15] We concluded that in spite of detected deviations up to 2.5 mm in the Pointer-WL tests, the addition of a 1 mm margin to the target volume was enough to ensure its dosage as was initially planned. It seems clear that analysis of the Pointer-WL test in terms of the ball center-radiation field distance does not necessarily agree with the actual shifts observed in the prescribed isodose line. Therefore, we think that dose-base shifts provide important dosimetric information in addition to simple geometrical deviations derived from a conventional Pointer-WL test. For instance, in a recent work of Adamson et al.,[16] the spatial accuracy of the delivered dose for multifocal SRS is quantified by measuring the shifts between the centroids of the planned and measured prescription dose volumes by using gel dosimetry.

As our linac does not have a 6D robotic couch able to correct rotational roll and tilt errors, the results of our study were obtained for CBCT-guided WL tests with just intentional translations. Although this be seen as a limitation of our study, similar results and conclusions would probably be obtained

if the rotational and translational intentional setup errors of the ball pointer were corrected using the CBCT scan.

5. Conclusions

We have proved that deviations greater than 1 mm as reported by the analysis of a conventional Pointer-WL test do not necessarily imply shifts greater than 1 mm in the prescription isodose line encompassing the target to be treated. We do believe that the dose-based geometric shift estimation given by the Dose-WL test described in our study is more clinically meaningful than a simple geometrical deviation derived from a traditional WL test. While the Pointer-WL test allows checking the spatial accuracy of the radiation isocenter and acting preventively to improve the mechanical movements, the Dose-WL test showed in the present study allows estimating the spatial accuracy of the prescription isodose line.

Conflict of interest

None declared.

Financial disclosure

None declared.

Acknowledgment

The authors thank Dr. M. Hermida-López for the suggestions and helpful comments he provided.

REFERENCES

1. Leksell L. The stereotaxic method and radiosurgery of the brain. *Acta Chirg Scand* 1951;**102**:316–9.
2. Deinsberger R, Tidstrand J. Linac radiosurgery as a tool in neurosurgery. *Neurosurg Rev* 2005;**28**(April (2)):79–88 [discussion 89–90, 91].
3. Lutz W, Winston KR, Maleki N. A system for stereotactic radiosurgery with a linear accelerator. *Int J Radiat Oncol Biol Phys* 1988;**14**(February (2)):373–81.
4. Hartmann GH, Bauer-Kirpes B, Serago CF, et al. Precision and accuracy of stereotactic convergent beam irradiations from a linear accelerator. *Int J Radiat Oncol Biol Phys* 1994;**28**(January (2)):481–92.
5. Verellen D, Soete G, Linthout N, et al. Quality assurance of a system for improved target localization and patient set-up that combines real-time infrared tracking and stereoscopic X-ray imaging. *Radiother Oncol* 2003;**39967**:129–41.
6. Chang J, Yenice KM, Narayana A, et al. Accuracy and feasibility of cone beam computed tomography for stereotactic radiosurgery setup. *Med Phys* 2007;**34**(June (6)):2077–84.
7. Jones J, Childress N, Kry S. Development of a modified Winston-Lutz test for evaluating errors in IGRT based setups. *Med Phys* 2011;**38**(July (6 Part11)):3505.
8. Zhang Q, Chan MF, Burman C, et al. Three independent one-dimensional margins for single-fraction frameless stereotactic radiosurgery brain cases using CBCT. *Med Phys* 2013;**40**(December (12)):121715.
9. Calvo JF, San José S, Garrido L, et al. Feasibility of an online adaptive replanning method for cranial frameless intensity-modulated radiosurgery. *Med Dosim* 2013;**38**(3):291–7.
10. Méndez I, Polsak A. The Multivariate Gaussian method: a new approach to multichannel radiochromic film. In: *8th AAPM Conf. Proc.*. 2017.
11. Palmer AL, Bradley DA, Nisbet A. Evaluation and mitigation of potential errors in radiochromic film dosimetry due to film curvature at scanning. *J Appl Clin Med Phys* 2015;**16**(2):5141.
12. Rasband WS. *ImageJ*. Bethesda, MD, USA: U.S. National Institutes of Health; 1997–2016 https://imagej.nih.gov/ij/.
13. Altman DG. *Practical statistics for medical research*. London: Chapman and Hall; 1996.
14. Ma L, Pinnaduwage D, McDermott M, et al. Whole-procedural radiological accuracy for delivering multi-session gamma knife radiosurgery with a relocatable frame system. *Technol Cancer Res Treat* 2014;**13**(October (5)):403–8.
15. Calvo Ortega JF, Wunderink W, Delgado D, et al. Evaluation of the setup margins for cone beam computed tomography-guided cranial radiosurgery: a phantom study. *Med Dosim* 2016;**41**(3):199–204 [Autumn].
16. Adamson J, Carroll J, Trager M, et al. Delivered dose distribution visualized directly with onboard kV-CBCT: proof of principle. *Int J Radiat Oncol Biol Phys* 2019;**103**(April (5)):1271–9.